Intelligent Manufacturing and Cloud Computing
I.S. Jesus and K. Wang (Eds.)

doi:10.3233/ATDE260274

Twin-Wire Arc Additive Manufacturing and Solution Treatment for NiTiNb Alloy: Phase Transformation, Microstructure, and Mechanical Property

Long Chen[a], Miao Zhao[a], Jiajia Shen[b], Fissha Biruke Teshome[a], Bowen Pang[a], Yiming Wu[a], Naixun Zhou[a] and Zhi Zeng[a,1]
[a]*School of Mechanical and Electrical Engineering, University of Electronic Science and Technology of China, Chengdu, 611731, China*
[b]*CENIMAT/I3N, Department of Materials Science, NOVA School of Science and Technology, Universidade NOVA de Lisboa, Caparica 2829-516, Portugal*

Abstract. NiTiNb shape memory alloys (SMAs) are attractive for applications that demand a wide transformation hysteresis. In this study, NiTiNb thin walls were fabricated using twin-wire arc additive manufacturing (T-WAAM) via in-situ co-feeding of NiTi and Nb wires, and the effect of subsequent solution treatment on phase transformation, microstructure, phase constitution, and mechanical property was systematically investigated. Both the as-deposited (AD) and solution-treated (HT) NiTiNb exhibit a significantly wider transformation hysteresis compared with NiTi wire. Solution treatment sharpens the transformation peaks, shifts the transformation to higher temperatures, and preserves the wide hysteresis. The AD state is characterized by directional dendritic structures and a continuous Nb-rich inter-dendritic network with a pronounced build-aligned texture. After solution treatment, this network decomposes into discrete Nb-rich particles, accompanied by improved chemical homogeneity, and texture weakening, without noticeable grain coarsening. Phase analysis indicates slightly intensified TiNb and minor Ti_2Ni formation, consistent with Nb partitioning from a supersaturated matrix. Mechanically, the AD state demonstrates slightly higher fracture strength but fails prematurely with reduced fracture strain, whereas the HT state shows modestly lower strength but enhanced ductility, consistent with fractographic observations. Overall, the combination of T-WAAM with an optimized solution treatment schedule effectively mitigates additive manufacturing-induced heterogeneity while maintaining the Nb-induced wide hysteresis, thereby providing a practical process rout for NiTiNb components with stable functional and mechanical performance.

Keywords. Twin-wire arc additive manufacturing, NiTiNb, Solution treatment, Microstructure, Phase transformation.

1. Introduction

NiTi-based shape memory alloys (SMAs) possess high specific strength, large recoverable strain, and excellent corrosion resistance, making them widely applicable

[1] Corresponding Author: Zhi Zeng, zhizeng@uestc.edu.cn

in biomedical engineering, adaptive structures, and energy-dissipation systems [1]. Their functional response arises from the thermoelastic B2↔B19' martensitic transformation, which is highly sensitive to composition as well as manufacturing-induced defects and precipitates [1, 2]. Within additive manufacturing (AM), laser powder bed fusion (LPBF) has clarified the coupled effects of build orientation, texture, and defects on pseudoelasticity and transformation temperatures in NiTi [3] However, LPBF also presents challenges, including elemental volatilization, composition drift, and melt pool-scale inhomogeneity heterogeneity, thereby requiring carefully designed thermal histories and post-processing to stabilize functional properties [4, 5].

NiTiNb ternary alloys have attracted substantial interest owing to the wide phase transformation hysteresis induced by Nb, which facilitates their potential for high damping and thermally driven actuation [6]. While this wide hysteresis is commonly associated with interfacial friction and elastic mismatch arising from secondary phases, it can also be achieved in single-phase NiTiNb, highlighting the combined influence of phase composition and solute distribution [7, 8]. In LPBF, in-situ alloying of pre-alloyed NiTi with elemental Nb was feasible, but the process frequently results in undissolved Nb or eutectic structures, which induce spatial variations in transformation and properties. Consequently, solution treatments are often employed to enhance chemical homogeneity and functional performance [9].

Wire-fed processes, such as wire arc AM (WAAM) and electron-beam AM (EBAM), complement powder-based approaches by offering higher deposition rates, simpler feedstock requirements, and precise in-situ composition control through multi-wire feeding [10, 11]. Early WAAM studies established the feasibility of fabricating NiTi components and revealed height-dependent variations in microstructure and phase transformation behavior [12]. More recently, wire-fed techniques have been extended to NiTiNb, where controllable secondary-phase morphologies, tunable transformation temperatures, and promising tensile properties have been reported following appropriate heat treatments [13, 14]. Within this context, twin-wire arc AM (T-WAAM) enables ternary in-situ alloying by co-feeding NiTi and Nb into a single molten pool. Existing studies demonstrated that T-WAAM can achieve uniform and wide transformation hysteresis [15]. Nevertheless, no studies have investigated the balance between phase transformation hysteresis and mechanical properties by regulating T-WAAM NiTiNb alloys through post-heat treatment.

In this study, T-WAAM is employed to fabricate NiTiNb walls using NiTi and Nb feedstock wires, followed by a comparative evaluation of phase transformation behavior, microstructure, phase constitution, and mechanical properties in the as-deposited (AD) and solution-treated (HT) states. The objective is to determine whether an appropriately designed solution treatment can homogenize Nb distribution, regulate second phases, and achieve a more coherent balance between transformation characteristics and mechanical property.

2. Experimental Method

A T-WAAM system equipped with an ultra-high-frequency pulsed TIG (UHFP-TIG) torch was employed to in-situ alloy NiTi with Nb, as illustrated in Figure 1(a). Commercial NiTi wire (50.5 at.% Ni) and high-purity Nb wire with 1.0 mm diameter were independently fed into the melt pool. To suppress oxidation, a coaxial nozzle and an argon-shielding device delivered high-purity argon at 15 L/min. Deposition was conducted under optimized parameters: peak current 210 A, base current 140 A, and torch travel speed 240 mm/min. The NiTi and Nb feed rates were set as 2200 mm/min and 260 mm/min, respectively, corresponding to a nominal Nb content of ~15 at.% in deposited wall. Further details of the platform configuration and process optimization can be found in our previous work [15]. To homogenize the microstructure, solution heat treatment was conducted in a furnace under a high-purity argon atmosphere. The samples were heated to 1000 °C, held for 30 min, and subsequently water quenched.

Following deposition, specimens for characterization and tensile testing were sectioned from the mid-height region of the wall, as shown in Figure 1(b). Phase transformation behavior was examined by differential scanning calorimetry (DSC) over the temperature range -70 °C to 120 °C at a heating/cooling rate of 10 °C/min under argon atmosphere. Microstructural features were analyzed using optical microscopy (OM) and scanning electron microscopy (SEM) equipped with energy-dispersive spectroscopy (EDS) and electron backscatter diffraction (EBSD). Phase constitution was identified by X-ray diffraction (XRD) within a 2θ range of 30°-80°. Mechanical properties were evaluated by uniaxial tensile testing at room temperature using an Instron 5548 micro-tensile testing machine at a displacement rate of 0.5 mm/min. Dog-bone-shaped specimens with gauge section of 12 mm × 2.5 mm × 1.0 mm were employed. Fracture surfaces were subsequently examined by SEM to identify failure modes.

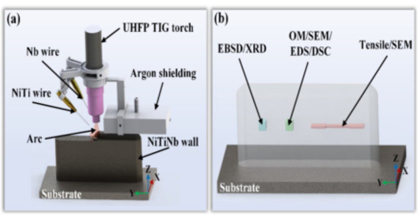

Figure 1. Schematic of T-WAAM fabricated NiTiNb wall: (a) experiment platform; (b) sample cutting position.

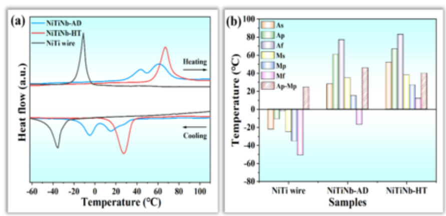

Figure 2. DSC results: (a) phase transformation curves; (b) phase transformation temperatures and hysteresis.

3. Results and Discussion

3.1. Phase Transformation

Figure 2 compares the DSC responses of the NiTi wire with those of the as-deposited (NiTiNb-AD) and solution-treated (NiTiNb-HT) alloys. The NiTi wire exhibits a single B2↔B19' phase transformation with a narrow hysteresis Ap-Mp (~24 °C) between the heating peak (Ap) and the cooling peak (Mp). By contrast, both NiTiNb conditions exhibit higher transformation temperatures together with a markedly wider hysteresis (~40°C - 46 °C). In the NiTiNb-AD state, the DSC curve shows a broadened peak with a weak pre-shoulder. Following solution treatment, the endothermic and exothermic peaks of NiTiNb-HT become sharper and shift to higher temperatures, while the hysteresis contracts slightly but remains substantially wider than that of NiTi.

The wider hysteresis of NiTiNb, relative to NiTi, originates from increased kinetic resistance during the forward/reverse phase transformations. First, Nb dissolved in the matrix enhances the elasticity and friction energy dissipation at the martensite/austenite interface, thereby requiring a higher driving force for transformation and significantly broadening the hysteresis [7]. Second, when secondary phases such as Nb-rich or eutectic structures are present, the strong elastic modulus and lattice mismatch across matrix/secondary-phase interfaces act as pinning sites, which introduces additional non-chemical energy dissipation during interface motion, further extending the thermal hysteresis [16]. The differences between NiTiNb-AD and NiTiNb-HT can be attributed to composition homogenization and stress relaxation induced by solution heat treatment. In the NiTiNb-AD state, the repeated thermal cycling inherent to T-WAAM leads to Nb segregation and Ni/Ti composition fluctuations, compounded by residual stresses, which together split and broaden the DSC peaks [6]. Solution treatment facilitates Nb redistribution and reduces local lattice distortion within the matrix, thereby sharpening the peaks and narrowing the spread of transformation temperatures [17].

3.2. Microstructure

Figure 3(a) (NiTiNb-AD) reveals pronounced directional solidification features, with an almost continuous inter-dendritic network. By contrast, Figure 3(e) (NiTiNb-HT) exhibits microstructural homogenization, where the previously continuous network is disrupted into island-like/short-rod-like features. No significant grain coarsening is observed at the optical scale, suggesting that the dominant effect of high-temperature treatment is solute redistribution and network disruption rather than substantial extensive grain growth. The orientation map of NiTiNb-AD in Figure 3(b) is dominated by columnar grains. Pole figures and inverse pole figures (IPF) in Figure 3(c) and (d) indicate a pronounced build-aligned texture, with a maximum texture intensity ~13. Following solution treatment (Figure 3(f)-(h)), the columnar morphology remains evident. However, the texture intensity decreases to ~8, and the IPF maps show a broader orientation distribution. The more uniformity of color contrast qualitatively reflects a reduction in preferred orientation, accompanied by a significant decrease in intra-crystalline misorientations, implying partial release of stored strain and relaxation of build-induced mismatch stress.

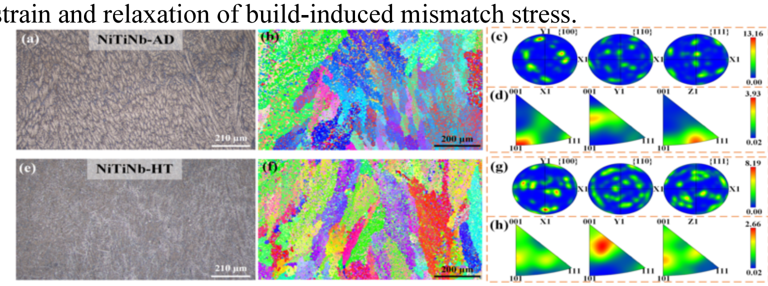

Figure 3. OM and EBSD characterization results of microstructure: (a)-(d) NiTiNb-AD; (e)-(h) NiTiNb-HT.

The strong texture in the as-deposited state accounts for the broadening and splitting of the DSC peaks. High residual elastic incompatibility within columnar grains raises the friction for grain boundary motion. Solution treatment promotes solute homogenisation and relieves internal stresses, thereby producing sharper endothermic/exothermic peaks and reducing transformation temperature dispersion. These observations are consistent with previous reports indicating that texture, combined with chemical heterogeneity, governs the transformation spread in WAAM-processed alloys [18].

3.3. Phase Analysis

For NiTiNb-AD, Figure 4(a)-(f) show a cellular/inter-dendritic network decorated by bright, particle-like phases. Nb EDS mapping confirms these bright features correspond to Nb-rich phases. The EDS line scan reveals periodic Nb peaks with corresponding Ni fluctuations and minor Ti variations, reflecting Nb segregation during solidification. Area-averaged compositions yield a Nb content of ~14.7 at.%, in good agreement with the nominal chemistry (~15 at.% Nb). After treatment, as shown in Figure 4(g)-(l), the bright Nb-rich network breaks into discrete equiaxed particles. The EDS line scan shows a sharp Nb increase accompanied by a corresponding Ni depletion. The area-averaged composition shifts slightly to Ti ≈ 50.5 at.%, Ni ≈ 35.4 at.%, and Nb ≈ 14.1 at.%, suggesting a modest reduction in the matrix Ni/Ti ratio due to solute diffusion. Morphologically, the transition from a quasi-continuous network to isolated particles represents the principal microstructural change induced by solution treatment.

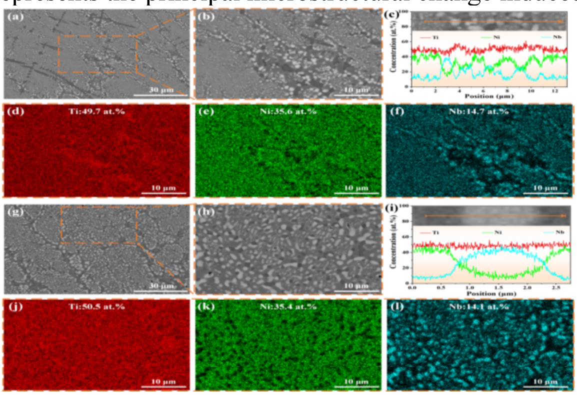

Figure 4. SEM and EDS characterization results: (a)-(f) NiTiNb-AD; (g)-(l) NiTiNb-HT.

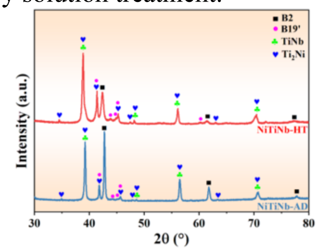

Figure 5. XRD diffraction pattern for NiTiNb-AD and NiTiNb-HT.

In Figure 5, both NiTiNb-AD and NiTiNb-HT exhibit predominant B2 diffraction peaks, accompanied by secondary reflections from TiNb and Ti_2Ni, as well as a weak B19' peak detectable at room temperature. The relative peak intensities evolve following solution treatment: (i) B2 peaks exhibit a slight shift, consistent with lattice distortion; and (ii) the TiNb and Ti_2Ni peaks become more pronounced, indicating precipitation and coarsening of Nb-rich and Ti-rich secondary phases from the supersaturated B2 matrix.

During T-WAAM, the large melting-point difference and limited diffusion time promote Nb segregation, leading to the forming of a continuous Nb-rich network. Solution treatment drives two key changes: (1) redistribution/precipitation - Nb diffuses out of supersaturated B2 and accumulates in TiNb; (2) homogenization - the network spheroidizes and fragmentates into discrete particles. The reduction in matrix Nb content and the release of lattice strain elevate the transformation temperature, while a slight decrease in the effective Ni/Ti ratio further increase the temperature [6].

3.4. Mechanical Property

In Figure 6(a), both conditions exhibit monotonic strain hardening without a distinct stress-induced transformation plateau, suggesting that dislocation slip dominates. NiTiNb-AD achieves a slightly higher fracture strength (σ_f) but fails prematurely with lower fracture strain (ε_f), whereas NiTiNb-HT exhibits a modestly reduced strength but enhanced ductility. According to Figure 6(b)-(c), the fracture surfaces of NiTiNb-AD predominantly characterized quasi-cleavage features with river patterns and cleavage steps, where precipitates are frequently observed at step intersections. After solution treatment, as shown in Fig. 6(d)-(e), quasi-cleavage still dominates, but fracture surfaces exhibit more tortuous crack paths, with shorter steps and fewer extended straight segments. These observations suggest that spheroidization and redistribution of Nb-rich regions disrupt crack propagation pathways, resulting in a more tortuous fracture trajectory.

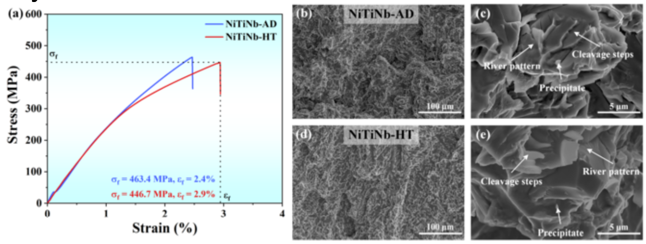

Figure 6. Tensile property: (a) stress-strain curves; fracture surface of (b)-(c) NiTiNb-AD; (d)-(e) NiTiNb-HT.

In T-WAAM, rapid thermal cycling produces a supersaturated B2 and a high density of stored strain. Both effects elevate the initial work-hardening rate and peak stress but also promote early crack nucleation along the continuous inter-dendritic network. Post-solution treatment homogenizes the matrix and partially relieves stored strain, leading to a modest reduction in strength accompanied by enhanced ductility, consistent with prior observations in AM-NiTi [19]. In the AD state, a Nb-rich network provides long-range constraints. The HT state breaks this network into discrete particles, thereby mitigating long-range constraints. This network-to-particle transition reduces the propensity for crack propagation and accounts for the higher fracture strain [2]. Such microstructure-property linkage aligns with previous reports that post-processing profoundly reshapes constraint pathways and mechanical response [20, 21]. Solution treatment reduces the matrix Nb content and slightly decreases the effective Ni/Ti ratio, shifting the transformation temperatures to higher values. However, a narrower distribution of local transformation temperatures after HT reduces load localization, improving ductility. Meanwhile, Nb- induced interfacial friction preserves the wide hysteresis [16].

4. Conclusion

This work investigated phase transformation, microstructure, phase, and mechanical property of T-WAAM NiTiNb and its solution-treated counterpart. DSC results confirm that both the AD and HT NiTiNb exhibit a significant wider transformation hysteresis than NiTi wire. Solution treatment shifts transformation to higher temperature, while the wide hysteresis is retained. The AD NiTiNb consists of a continuous Nb-rich inter-dendritic network and a pronounced build-aligned texture. After solution treatment, this network breaks into discrete Nb-rich particles, chemical homogeneity improves, texture weakens, and second-phase precipitation increases. The AD state achieves slightly higher strength but lower ductility, whereas the HT state shows a small strength decrease but enhanced elongation. Fractography analysis reveals a transition from long, network-guided quasi-cleavage in AD to a more tortuous path after HT.

5. Acknowledgments

This work is supported by the National Natural Science Foundation of China (Nos. 52175292, 52405395), and Science and Technology Project of Sichuan Province (No. 2023ZDZX0003).

References

[1] Wei, S. S., Zhang, J. L., Zhang, L., et al., "Laser powder bed fusion additive manufacturing of NiTi shape memory alloys: a review," International Journal of Extreme Manufacturing, 5(3), 032001 (2023).
[2] Elahinia, M., Moghaddam, N. S., Andani, M. T., et al., "Fabrication of NiTi through additive manufacturing: A review," Progress in Materials Science, 83, 630-663 (2016).
[3] Safaei, K., Nematollahi, M., Bayati, P., et al., "On the crystallographic texture and torsional behavior of NiTi shape memory alloy processed by laser powder bed fusion: Effect of build orientation," Additive Manufacturing, 59, 103184 (2022).
[4] Yin, J., Zhang, W. Q., Ke, L. D., et al., "Vaporization of alloying elements and explosion behavior during laser powder bed fusion of Cu-10Zn alloy," International Journal of Machine Tools & Manufacture, 161, 103686 (2021).
[5] Wen, S. F., Liu, Y., Zhou, Y., et al., "Effect of Ni content on the transformation behavior and mechanical property of NiTi shape memory alloys fabricated by laser powder bed fusion," Optics and Laser Technology, 134, 106653 (2021).
[6] Fan, Q. C., Zhang, Y., Zhang, Y. H., et al., "Influence of Ni/Ti ratio and Nb addition on martensite transformation behavior of NiTiNb alloys," Journal of Alloys and Compounds, 790, 1167-1176 (2019).
[7] Kang, G. F., Zhang, H., Ma, Z. Y., et al., "Large thermal hysteresis in a single-phase NiTiNb shape memory alloy," Scripta Materialia, 212, 114574 (2022).
[8] Polozov, I., Popovich, A., "Microstructure and Mechanical Properties of NiTi-Based Eutectic Shape Memory Alloy Produced via Selective Laser Melting In-Situ Alloying by Nb," Materials, 14(10), 2696 (2021).
[9] Xi, R., Jiang, H., Li, G. C., et al., "Effect of solution treatment on the microstructure, phase transformation behavior and functional properties of NiTiNb ternary shape memory alloys fabricated via laser powder bed fusion alloying," International Journal of Extreme Manufacturing, 6(4), 045002 (2024).
[10] Zeng, Z., Cong, B. Q., Oliveira, J. P., et al., "Wire and arc additive manufacturing of a Ni-rich NiTi shape memory alloy: Microstructure and mechanical properties," Additive Manufacturing, 32, 101051 (2020).
[11] Osipovich, K., Kalashnikov, K., Chumaevskii, A., et al., "Wire-Feed Electron Beam Additive Manufacturing: A Review," Metals, 13(2), 279 (2023).
[12] Han, J., Chen, X. Y., Zhang, G. Y., et al., "Microstructure and Mechanical Properties of NiTi Alloy Prepared by Double-Wire plus Arc Additive Manufacturing Plus Heat Treatment," 3d Printing and Additive Manufacturing, 11(3), 1008-1015 (2024).
[13] Xu, M. F., Chen, Y. H., Zhang, T. M., et al., "Wire-based electron beam additive manufacturing of NiTiNb shape memory alloy: Microstructure, phase-transformation behavior and mechanical properties," Materials Science and Engineering: A, 901, 146509 (2024).
[14] Pu, Z., Chen, C. Y., Du, D., et al., "Accelerated improvement in tensile superelasticity of electron beam directed energy deposition manufactured NiTi alloys by artificial thermal cycling combined with low temperature aging treatment," Virtual and Physical Prototyping, 19(1), e2352782 (2024).
[15] Chen, L., Zhao, M., Wu, J. H., et al., "Achieving uniform and wide phase transformation hysteresis in twin-wire arc additive manufactured NiTiNb alloy," Materials Research Letters, 13(8), 854-862 (2025).
[16] Hamilton, R. F., Lanba, A., Ozbulut, O. E., et al., "Shape Memory Effect in Cast Versus Deformation-Processed NiTiNb Alloys," Shape Memory and Superelasticity, 1(2), 117-123 (2015).
[17] Shu, X. Y., Lu, S. Q., Li, G. F., et al., "Nb solution influencing on phase transformation temperature of Ni47Ti44Nb9 alloy," Journal of Alloys and Compounds, 609, 156-161 (2014).

[18] Chen, L., Oliveira, J. P., Yan, X., et al., "Microstructure and Phase Transformation Behavior of NiTiCu Shape Memory Alloys Produced Using Twin-Wire Arc Additive Manufacturing," Additive Manufacturing Frontiers, 3, 200132 (2024).
[19] Tareq, S., Rahman, T., Poudel, B., et al., "Heat treatment protocol for additively manufactured nitinol shape memory alloys in biomedical applications," Materials Science and Engineering: A, 897, 146274 (2024).
[20] Li, K., Ma, R. J., Zhan, J. B., et al., "Insight into the cracking mechanism of super-elastic NiTi alloy fabricated by laser powder bed fusion," Virtual and Physical Prototyping, 19(1), e2368654 (2024).
[21] Chen, L., Zhao, M., Wu, J. H., et al., "Mechanical property strengthening by post-heat treatments in NiTiCu shape memory alloys fabricated by twin-wire arc additive manufacturing," Virtual and Physical Prototyping, 20(1), e2457579 (2025).